Delayed feedback induced multirhythmicity in the oscillatory electrodissolution of copper

Timea Nagy, Erika Verner, Vilmos Gáspár, Hiroshi Kori, and István Z. Kiss

Citation: Chaos: An Interdisciplinary Journal of Nonlinear Science **25**, 064608 (2015); doi: 10.1063/1.4921694
View online: http://dx.doi.org/10.1063/1.4921694
View Table of Contents: http://scitation.aip.org/content/aip/journal/chaos/25/6?ver=pdfcov
Published by the AIP Publishing

Delayed feedback induced multirhythmicity in the oscillatory electrodissolution of copper

Timea Nagy,[1,2] Erika Verner,[2] Vilmos Gáspár,[2] Hiroshi Kori,[3] and István Z. Kiss[1]
[1]*Department of Chemistry, Saint Louis University, 3501 Laclede Ave., St. Louis, Missouri 63103, USA*
[2]*Department of Physical Chemistry, University of Debrecen, Egyetem tér 1, 4032 Debrecen, Hungary*
[3]*Department of Information Sciences, Ochanomizu University, 2-1-1 Ohtsuka, Bunkyo-ku, Tokyo 112-8610, Japan*

(Received 9 March 2015; accepted 30 April 2015; published online 28 May 2015)

Occurrence of bi- and trirhythmicities (coexistence of two or three stable limit cycles, respectively, with distinctly different periods) has been studied experimentally by applying delayed feedback control to the copper-phosphoric acid electrochemical system oscillating close to a Hopf bifurcation point under potentiostatic condition. The oscillating electrode potential is delayed by τ and the difference between the present and delayed values is fed back to the circuit potential with a feedback gain K. The experiments were performed by determining the period of current oscillations T as a function of (both increasing and decreasing) τ at several fixed values of K. With small delay times, the period exhibits a sinusoidal type dependence on τ. However, with relatively large delays (typically $\tau \gg T$) for each feedback gain K, there exists a critical delay τ_{crit} above which birhythmicity emerges. The experiments show that for weak feedback, $K\tau_{crit}$ is approximately constant. At very large delays, the dynamics becomes even more complex, and trirhythmicity could be observed. Results of numerical simulations based on a general kinetic model for metal electrodissolution were consistent with the experimental observations. The experimental and numerical results are also interpreted by using a phase model; the model parameters can be obtained from experimental data measured at small delay times. Analytical solutions to the phase model quantitatively predict the parameter regions for the appearance of birhythmicity in the experiments, and explain the almost constant value of $K\tau_{crit}$ for weak feedback. © *2015 AIP Publishing LLC*.
[http://dx.doi.org/10.1063/1.4921694]

Although all isolated systems tend towards a unique, stationary state (thermodynamic equilibrium state), open systems can exhibit multiple states, whose realization depends on the initial condition. In chemical systems, multiplicity is often observed with stationary states, or with a single oscillatory and many stationary states. Nonetheless, multiplicity can also occur with oscillatory chemical reactions, where depending on initial conditions, two different types of oscillations can be obtained. Such birhythmicity can often be observed with two coupled chemical systems, where different synchronization patterns could produce different periods for the oscillatory cycles. However, another form of birhythmicity can also be observed when a single oscillatory chemical reaction is coupled to "itself" through a sufficiently large delay via a self-feedback mechanism. This paper explores the emergence of such multirhythmic dynamics with an electrochemical reaction (Cu electrodissolution in phosphoric acid) where the measured electrode potential, which determines the rate of the dissolution, is fed back with a delay to the circuit potential, which drives the dissolution reaction. Through experiments, numerical simulations, and a phase-model analysis, we show that the feedback mechanism can provide an efficient way for generating robust, finely tuned periods for the oscillations. Such mechanism could be implemented to construct versatile timers in biological and engineering applications.

I. INTRODUCTION

Systems of rhythmic processes often interact with the environment in a complex manner, and changes induced in the environment, in turn, affect the inherent dynamics of the system. One approach to a simplified description of such systems is based on the application of delayed differential equations. Examples include physiological systems,[1] metabolic feedback to circadian system,[2] or laser dynamics.[3] Delayed feedback is also a fundamental method by which control of complex dynamics can be achieved.[4–6] In chemical systems, delayed feedback was applied to a variety of simple oscillatory and chaotic systems[7,8] in homogenous reactions,[9,10] heterogeneous catalysis,[11] and electrochemical systems.[12] Chaotic systems were controlled,[10,11,13,14] spiral waves were tamed,[15] synchronous behavior was finely tuned,[16] and clustering and other types of complex spatiotemporal structures were induced[17–20] by the delayed feedback.

Comprehensive theoretical treatment of delayed equations is a challenging task; however, phase and Stuart-Landau models provide an efficient framework for description of oscillatory behavior as a function of feedback delay

and strength.[16,21,22] Analytical studies about the period of oscillations predicted possible occurrence of *birhythmicity* (co-existence of two stable periodic orbits) with relatively strong feedback and with a large delay.[21,22] With weak feedback and small delay, the period of oscillations changes as a function of feedback delay in a harmonic manner; however, at large coupling strength/delay, the harmonic shape transforms to a Z-shape creating two stable and one unstable periodic orbits with different periods at the same feedback delay. Theoretical predictions also showed that the number of stable periodic solutions grows as delay increases.[21] Feedback induced birhythmicity was found in experiments with the minimal bromate oscillator in a continuous flow stirred tank reactor.[23] Indication of birhythmicity (discontinuous and abrupt change of period as a function of feedback gain) was also found in CO oxidation on Pt with externally imposed feedback.[24] We note that birhythmicity can also appear without any apparent external feedback; for example, in a system of coupled bromate oscillators,[25] in the hydrogen-oxygen reaction in a continuous-flow reactor at low pressures,[26] and in models of glycolytic oscillations.[27] In these systems, the origin of birhythmicity is related to some positive or negative feedbacks that are inherent in the system.

In this paper, we investigate an oscillating electrochemical process (the electrodissolution of copper in phosphoric acid electrolyte[28,29]) under the effect of externally imposed delayed feedback in order to explore the dynamical features as a function of both the feedback gain and delay. We have chosen an electrochemical process because of the possibility of extensive experimental characterizations with delayed feedback;[29] in addition, phase model descriptions (with relatively small delay) have been successful in describing the dynamics of synchronization of electrochemical oscillators.[30] The system thus allows us to test to what extent a phase model description can be applied to predicting the appearance of multirhythmicity in an experimental system at small and large values of feedback delays (e.g., multiple times the oscillatory period of the unperturbed, autonomous system).

The paper is structured as follows. We start with showing the characteristics of delay induced birhythmicity that emerges in a general model for current oscillations during metal electrodissolution. Then a simple phase model is constructed to characterize the observed dynamics. We derive a relationship between the feedback gain and the critical delay at which birhythmicity may occur. Finally, experimental results are shown that verify the "birth" of birhythmicity at the predicted values of feedback gain and delay; in addition, experimental evidence for the appearance of an even higher order multirhythmicity (i.e., trirhythmicity) is also presented.

II. RESULTS AND DISCUSSION

A. Feedback induced birhythmicity in a general model for metal electrodissolution: Numerical results

For understanding the emergence of delay induced multirhythmicity in an oscillating electrochemical system, we consider the following general model for a negative differential resistance (N-NDR) type electrochemical oscillator, such as the Cu-o-phosphoric acid system:[31]

$$\frac{de}{dt} = \frac{v-e}{r} - 120\xi(e)u, \tag{1}$$

$$\frac{du}{dt} = -1.25d^{1/2}\xi(e)u + 2d(w-u), \tag{2}$$

$$\frac{dw}{dt} = 1.6d(2-3w+u). \tag{3}$$

In Eqs. (1)–(3), e is the dimensionless electrode potential, u is the dimensionless concentration of an electroactive species in the near-surface diffusional layer (Nernst layer), w is the dimensionless concentration of the *same* electroactive species in the secondary diffusional layer, while t is dimensionless time. Equation (1) defines the charge balance during the anodic process, Eq. (2) is the reaction-diffusion equation for the electroactive species in the Nernst layer, while Eq. (3) gives the change in the concentration (w) due to only diffusion between the layers. Further details of the model, including exact definitions of the dimensionless variables, are described by Koper and Gaspard.[31]

The dimensionless parameters of the model are the total series resistance r, the circuit potential v, the rotation rate d, and the potential dependent rate constant ξ(e) for the N-NDR system[31,32]

$$\xi(e) = 2.5\,\Theta^2 + 0.01\exp[0.5\,(e-30)], \tag{4}$$

where Θ is the surface coverage of the electrode

$$\Theta = \left\{ \begin{array}{ll} 1 & \text{if } e \le 35 \\ \exp\left[-0.5(e-35)^2\right] & \text{if } e > 35 \end{array} \right\}. \tag{5}$$

We note that Eqs. (1)–(3) are considered as a general kinetic model for a class of electrochemical oscillations. In this model, positive feedback to the electrochemical reaction in Eq. (1) is caused by the negative differential resistance (decreasing current with increasing electrode potential) due to some inhibiting chemical process. This positive feedback, when combined with a slow negative feedback caused by diffusion is the source of the instability that may lead to oscillations. In the original derivation of the equations, the electroactive species was In^{3+} ion, while the negative differential resistance was caused by the desorption of the catalyst, SCN^-, with coverage Θ.[31,32]

In this work, we use Eqs. (1)–(3) to demonstrate the effect of feedback to the wide class of electrochemical oscillations generated by N-NDR mechanism. During copper electrodissolution at large overpotential, where the oscillations occur, the limiting current is due to the diffusion of water to the electrode;[33,34] therefore, when the general model of electrochemical oscillations (Eqs. (1)–(3)) is applied to copper electrodissolution, u and w may correspond to water concentrations in the diffusional layers. The inhibiting step causing N-NDR kinetic features is likely related to the formation of copper oxides[35] on the electrode surface. The validity of Eqs. (1)–(3) has been extensively verified for description the dependence of oscillatory features, for

example, on series resistance, electrode size and capacitance, and rotation rate of the disk.[12,36–38] For our calculations here, we chose parameter values that set the system close to a Hopf bifurcation point in the bifurcation diagram and apply a delayed feedback.

For simulations, we applied the differential delayed feedback (DDF) formula introduced by Pyragas[4] as follows. The circuit potential is set by a real time controller

$$v(t) = v_0 + \delta v(t), \tag{6}$$

where v_0 is the dimensionless base (constant) circuit potential when no feedback is applied, and δv(t) is the potential perturbation (feedback) calculated as follows:

$$\delta v(t) = k[e(t) - e(t-\tau)], \tag{7}$$

where k and τ are the feedback gain and delay, respectively. Without feedback, the calculated current oscillations have an angular frequency $\Omega = (2\pi/T) = 4.25$. The effect of feedback (with gain $k = 0.05$) on the frequency is shown in Figure 1. The value of τ has been varied between 0 and 10; for each simulation, the initial conditions were taken from the last point of the preceding one.

Birhythmicity (the coexistence of two oscillatory solutions with different periods) can be detected by the following procedure (Figure 1): the delay time τ first is increased from 0 to 10 in an upward scan then it is decreased back to 0 in the backward scan, both under control. The upper branch (backward scan) can be approached by an appropriate parameter perturbation (for example, slightly changing v) of the lower branch. Note that for relatively large delay, there appears a "splitting," and no overlapping is possible for the forward and backward scans. The figure also indicates that by increasing the delay time, the width of the hysteresis loops increases.

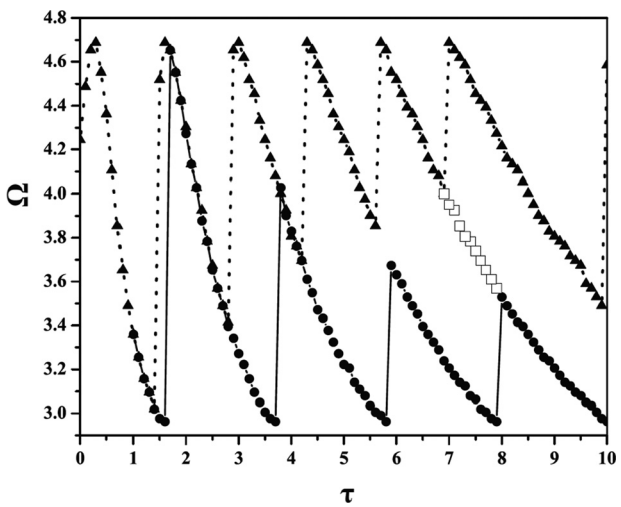

FIG. 1. Simulations with kinetic model: dynamical birhythmicity and trirhythmicity. Birhythmicity and trirhythmicity are shown in the angular frequency Ω (=2π/T) vs. delay time τ plot. The delay time τ is first increased (●) then decreased back (▲) while control is applied with $k = 0.05$ at $v_0 = 36.6909$, $r = 0.02856$, and $d = 0.11913$. Trirhythmicity exists between $\tau = 6.8$ and 8. The middle branch can be approached by slightly perturbing the oscillating system at the upper or lower branches, then it can be traced by either increasing or decreasing the delay time τ.

With relatively large delay, trirhythmicity can be observed. It is the result of the coexistence of three periodic solutions. It means that there exist three limit-cycles with different periods in the phase space of the system. The middle branch can be approached by slightly perturbing the oscillatory system at either the upper or the lower branches. The periodic oscillations of the middle branch can then be traced by either increasing or decreasing the delay time.

These numerical results are consistent with the results of previous analytical studies and numerical modeling with general model equations.[21,22] Our present numerical modeling predicts that multirhythmic behavior may occur in the experimental system, when the feedback is constructed from the oscillating electrode potential, while the control (perturbed) parameter is the circuit potential.

B. Phase model interpretation of multirhythmicity

For a deeper understanding of the laws of dynamics resulting in the emergence of multirhythmicity, we now analyze a general phase model[39] of an oscillating system subject to a weak feedback. The phase dynamics can be described as follows:

$$\frac{d\Phi(t)}{dt} = \omega + \kappa f(\Phi(t) - \Phi(t-\tau)), \tag{8}$$

where $\Phi(t)$ is the phase, t is time, ω is the natural angular frequency of the oscillations, $\kappa \geq 0$ and $\tau \geq 0$ are, respectively, the feedback gain and delay, while f is the functional form of the feedback. For a system close to a Hopf bifurcation point (where the waveform of oscillations is almost sinusoidal), this function–by considering a simple proportional feedback[40]–can be given as follows:

$$f(\Phi) = \sin(\Phi + \alpha) - \sin(\alpha), \tag{9}$$

where α is a parameter that depends on the type of oscillations. In the given example, the effect of α on the observed dynamics is small; therefore, we consider $\alpha = 0$, thus we can write

$$\frac{d\Phi(t)}{dt} = \omega + \kappa \sin(\Phi(t) - \Phi(t-\tau)). \tag{10}$$

Equation (10) has a periodic solution $\Phi(t) = \Omega t$ with a constant angular frequency $\Omega = 2\pi/T$ (where T is the period of oscillations) satisfying the following relation:

$$\Omega = \omega + \kappa \sin(\Omega\tau) \equiv g(\Omega). \tag{11}$$

In general, there might be multiple solutions to this implicit equation depending on ω, κ, and τ. For sufficiently small τ, there is only one solution, and the system exhibits oscillations with the given value of the angular frequency only. However, by increasing the delay time τ, a pair of new solutions may appear via a saddle-node bifurcation at a critical delay time τ_{crit}. Such a saddle-node bifurcation can result in birhythmicity, and further saddle-node bifurcations of the periodic solutions can bring about even higher order multirhythmicities.

The frequency of the solution at the critical point can be obtained by realizing that at the saddle-node bifurcation, $dg(\Omega)/d\Omega = 1$, therefore,

$$\kappa\tau_{crit}\cos(\Omega\tau_{crit}) = 1. \tag{12}$$

Because $\cos(\Omega\tau_{crit}) \leq 1$, we can define a lower bound condition that should be satisfied for the emergence of the bifurcation

$$1 \leq \kappa\tau_{crit}. \tag{13}$$

By further increasing τ to τ^* ($\tau^* > \tau_{crit}$), there will be a new solution at which $\Omega = \omega$; at this point

$$\omega\tau^* = 2n^*\pi, \tag{14}$$

where n^* is the minimum integer that satisfies $\kappa\, 2n^*\,\pi\,/\omega \geq 1$. Therefore,

$$\kappa\tau^* = \kappa\frac{2n^*\pi}{\omega}. \tag{15}$$

The value of τ^* provides an upper bound for the bifurcation. By the combination of Eqs. (13) and (15), we can define the lower and upper bounds for τ values at which birhythmicity may occur

$$1 \leq \kappa\tau_{crit} \leq \kappa\frac{2n^*\pi}{\omega}. \tag{16}$$

For very weak feedback (κ is small), n^* must be large, so that the upper bound is approximately unity for any small κ value; therefore,

$$\kappa\tau_{crit} \approx 1. \tag{17}$$

Equation (17) implies that at the critical value, where birhythmicity appears, the product of the feedback gain and delay is nearly a constant value. When the feedback gain is increased, the upper bound of $\kappa\tau_{crit}$ will increase unless

$$2(n* - 1)\pi\kappa/\tau_{crit} < 1, \tag{18}$$

i.e.,

$$n^* < \frac{\omega}{2\pi\kappa} + 1. \tag{19}$$

By substituting Eq. (19) into Eq. (15), we obtain an approximate formula for the dependence of feedback strength κ of the upper bound on the critical feedback delay τ_{max}:

$$1 + \kappa\frac{2\pi}{\omega} \equiv \kappa\tau_{max}. \tag{20}$$

Analytical predictions of the phase model are confirmed by numerical simulations using Eq. (10) with $\omega = 8.2$ rad/s (see Figure 2). This angular frequency is similar to the experimentally observed frequencies of the electrochemical oscillations. Witch increasing τ (at $\kappa = \pi/6$ in panel a), the angular frequency Ω initially changes in a sinusoidal manner; however at large delays, the variation is distorted, and the overlapping of two branches of periodic solutions indicates the presence of birhythmicity. In this example, the first bifurcation resulting in birhythmicity occurs at $\tau_{crit} = 2.3$ s, as expected from the theory ($1\,\text{rad} \leq \kappa\,\tau_{crit} \leq 1.20$ rad; the upper bound is calculated from Eq. (16) with $n^* = 3$). Note that in the phase model, we define the unit of κ as rad/s. For large delay ($\tau > 9.5$ s), similar to the experiments, trirhythmicity can occur because of the overlapping of multiple curves of periodic solutions. Common points of the two functions in Eq. (11), Ω, and $g(\Omega)$ exist in the range of $\omega - \kappa \leq \Omega \leq \omega + \kappa$. The number of common points (that gives the degree of multirhythmicity) increases with τ, and the multiplicity of solutions can be roughly estimated by considering the difference Δ of the phases ($\Omega\tau$) between the edges, i.e., $\Delta = (\omega + \kappa)\,\tau - (\omega - \kappa)\,\tau = 2\kappa\tau$. The degree of multiplicity increases when Δ is increased approximately by 2π. This corresponds to an increase in τ by π/κ, which is 6 s for $\kappa = \pi/6$. In Figure 2(a), birhythmicity occurs at $\tau_{crit} = 2.3$ s, while trirhythmicity at 9.5 s, which is close to the expected value ($\tau_{crit} + 6 = 8.3$ s).

Figure 2(b) shows that the numerically determined value of the critical delay for birhythmicity decreases with increasing the coupling strength, as it is expected from Eq. (16). The same data are applied to plot $\kappa\tau_{crit}$ vs. κ in Figure 2(c). Since the feedback gain is relatively small, all values are close to $\kappa\tau_{crit} \approx 1$. The larger $\kappa\tau_{crit}$ values (where n^* changes by 1) align with the theoretically predicted Eq. (20).

We have shown that simple geometric arguments can explain the appearance of bi- and trirhythmicities, and the phase model can be applied to predict the critical feedback delays where the bifurcations occur. We note that the feedback gains in the phase model (κ) and in the experiments (K) are quantities that differ only by a constant multiplier. For simplicity, we suppose that $\kappa = \beta K$, therefore, the lower bound condition for the appearance of birhythmicity in the experiments can be defined as follows:

$$\kappa\tau_{crit} = \beta K\tau_{crit} = 1 \rightarrow K\tau_{crit} = \frac{1}{\beta}. \tag{21}$$

The conversion factor β can be determined experimentally at small values of τ, where birhythmicity does not appear yet. For small τ, the solutions for Ω in Eq. (11) are sinusoidal functions of τ. Since the difference between the maximal and minimal values of angular frequencies is defined as follows:

$$\Delta\Omega = \Omega_{max} - \Omega_{min} = 2\kappa = 2\beta K, \tag{22}$$

the lower bound condition $K\tau_{crit} = 1/\beta$ in the experiments can be determined (and predicted) as the slope of a straight line fitted to experimental data (plotted as $\Delta\Omega$ vs. K).

C. Experimental results

A standard three-electrode electrochemical cell was applied to study the dynamics of current oscillations during the electrodissolution of copper in o-phosphoric acid electrolyte under potentiostatic condition without and with feedback. The reference electrode was either a saturated calomel or Hg/Hg_2SO_4/sat. K_2SO_4 electrode, the counter electrode was a Radelkis OH-9437 Pt-sheet electrode (area 5 cm^2), and

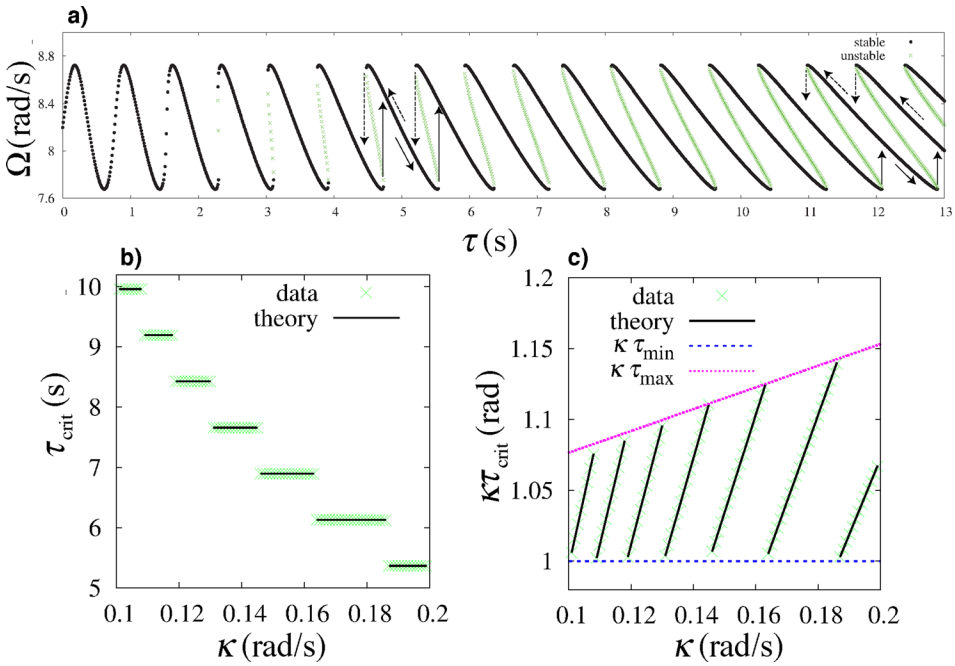

FIG. 2. Phase model simulations: birhythmicity and trirhythmicity. (a) Angular frequency Ω vs. feedback delay τ in the phase model with $\omega = 8.2$ rad/s and $\kappa = \pi/6$. Arrows indicate expected transitions between the lower and upper branches of the oscillations by increasing and decreasing τ in the given range. (b) Critical delay τ_{crit} at which birhythmicity first appears as a function of feedback gain κ. It has been determined numerically from sets of simulations similar to those in panel (a). (c) Dependence of $\kappa\tau_{crit}$ on feedback gain κ calculated from data of panel (b). The plotted lines show the theoretically predicted values for minimal and maximal delay times calculated, respectively, according to Eqs. (17) and (20).

the working electrode was a rotating copper disk (99.99%, diameter 5 mm, rotation rate 1500 rpm). All potentials are given with respect to the Hg/Hg_2SO_4/sat. K_2SO_4 electrode. In all experiments, we applied 70 ml 85% o-phosphoric acid at constant temperature (20 ± 0.1 °C).

A computer controlled potentiostat (Electroflex EF451) was applied to set the circuit potential (resolution 0.01 mV) between the working and reference electrodes. An adjustable external resistor in series with the working electrode was applied to provide the ohmic drop necessary for the appearance of current oscillations. Unless otherwise stated, the resistance was set to $R = 85\,\Omega$. The current I was measured with an ammeter (accuracy: 0.001 mA) built in the potentiostat. The sampling frequency for data acquisition was 200 Hz. Further details about the experiments can be found in our previous reports.[13,14]

Delayed-feedback is applied to the circuit potential V(t) using the electrode potential E(t) calculated as follows:

$$E(t) = V(t) - I(t)R. \tag{23}$$

The circuit potential is set by a real time controller

$$V(t) = V_0 + \delta V(t), \tag{24}$$

where V_0 is the base circuit potential when no feedback is applied and δV(t) is the potential perturbation (feedback) calculated as follows:

$$\delta V(t) = K[E(t) - E(t-\tau)], \tag{25}$$

where K and τ are the feedback gain and delay time, respectively. Experiments have been carried out to determine the angular frequency $\Omega = 2\pi/T$ (rad/s) of the oscillating current as a function of K and τ.

Figure 3 shows typical smooth oscillations ($T_0 = 0.79$ s) of current I and electrode potential E when no feedback is applied (autonomous system). In the experiments, the circuit

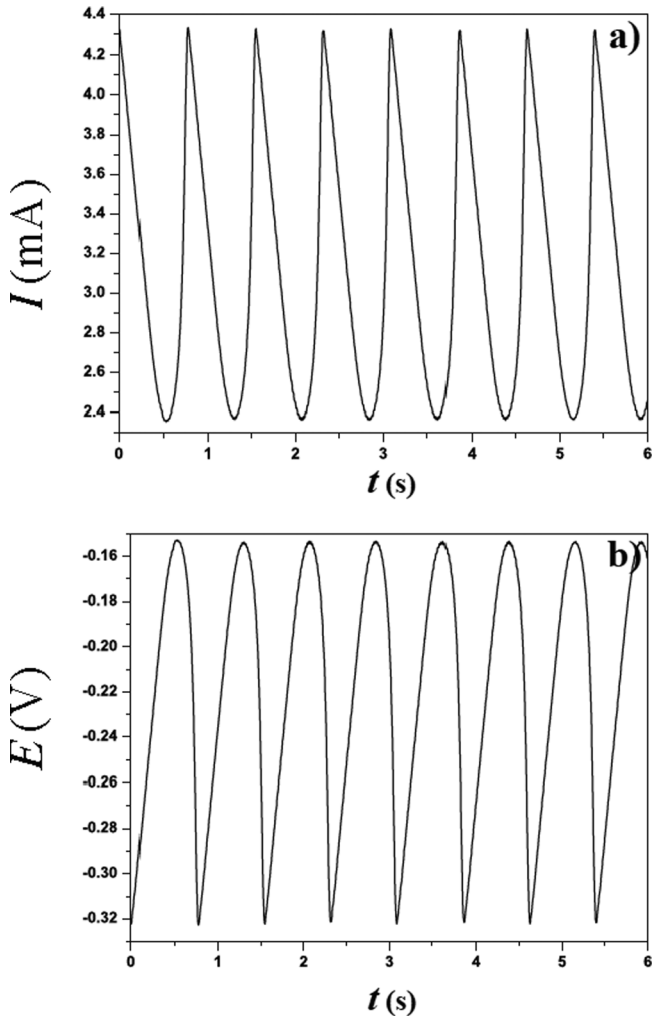

FIG. 3. Experiments: Oscillations of the system without feedback. Typical smooth oscillations of (a) the current I and (b) the electrode potential E in the o-phosphoric acid electrolyte/rotating disk copper electrode system without feedback ($K = 0$). The measured period of oscillations is $T_0 = 0.79$ s. The applied circuit potential is $V_0 = 64$ mV, slightly above the potential where the Hopf bifurcation occurs ($V_H = 54$ mV).

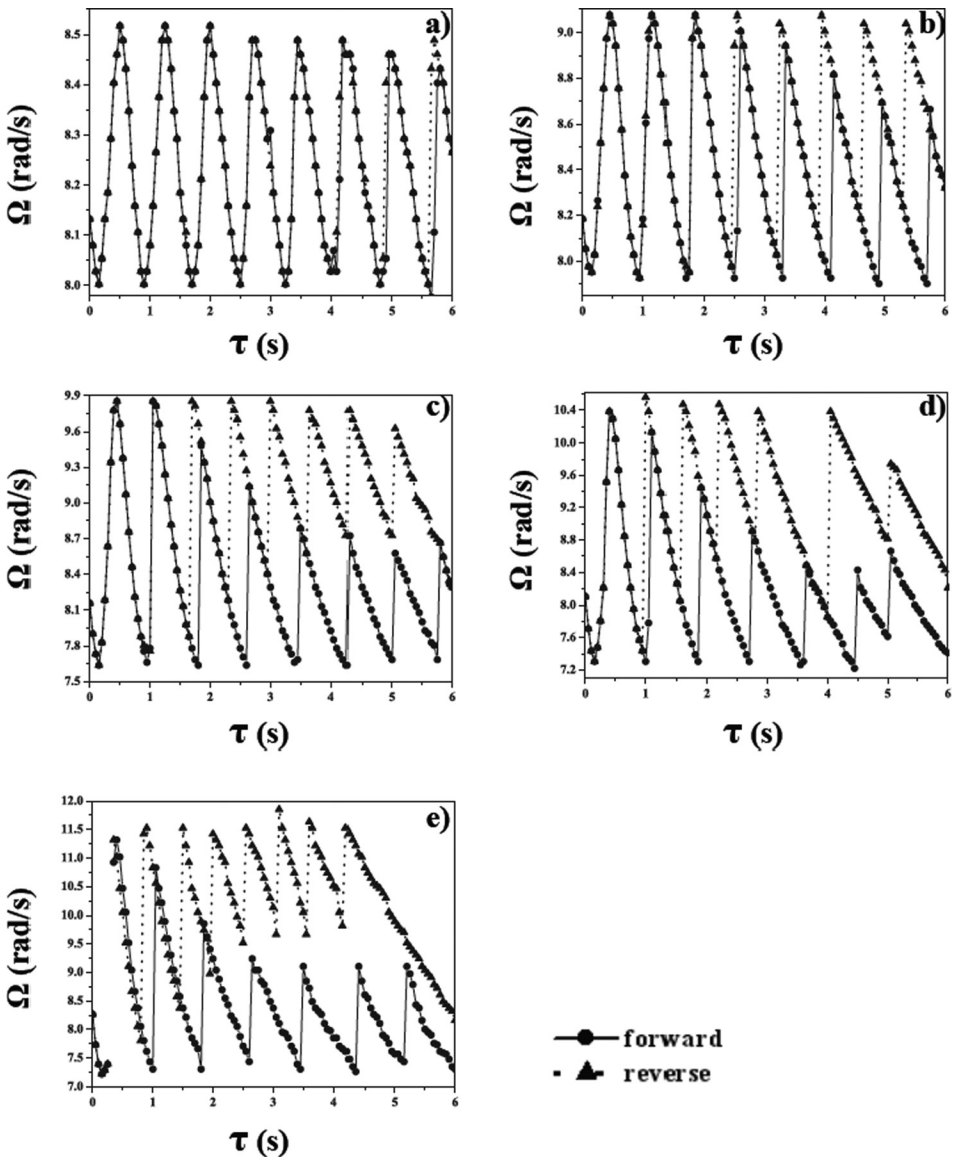

FIG. 4. Experiments: delayed-feedback induced birhythmicity. Angular frequency of oscillations Ω at different control gains K when the delay time τ is first increased stepwise (●) from 0 to 6 s then decreased back to 0 (▲). Note that the critical delay time τ_{crit} for the first appearance of birhythmicity decreases as the control gain is increased: (a) $K=0.01$, $\tau_{crit}=4.85$ s, $V_H=40$ mV, $V_0=50$ mV, $R=86$ Ohm; $T_0=0.77$ s. (b) $K=0.02$, $\tau_{crit}=2.5$ s, $V_H=54$ mV, $V_0=64$ mV, $R=85$ Ohm; $T_0=0.77$ s. (c) $K=0.04$, $\tau_{crit}=1.5$ s, $V_H=54$ mV, $V_o=64$ mV, R = 85 Ohm; $T_o=0.77$ s. (d) K = 0.06, $\tau_{crit}=1$ s, $V_H=54$ mV, $V_0=64$ mV, R = 85 Ohm; $T_0=0.78$ s. (e) $K=0.08$, $\tau_{crit}=0.9$ s, $V_H=40$ mV, $V_0=50$ mV, $R=86$ Ohm; $T_0=0.76$ s. At $\tau=0.3$ s, amplitude death (AD) is observed.

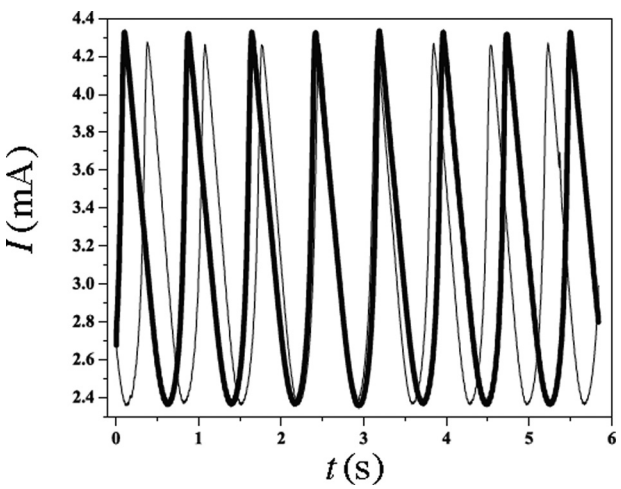

FIG. 5. Experiments: current oscillations during birhythmicity. Periodic current oscillations in the range of birhythmicity at $V_0=64$ mV ($V_H=54$ mV) with control gain $K=0.02$ (see Figure 4(b)) and feedback delay $\tau=4.7$ s. Thick curve shows the current oscillations ($T=0.79$ s) observed during the forward scan of τ, while the thin curve shows the current oscillations ($T=0.71$ s) observed during reverse scan of τ.

potential was set by the potentiostat ($V_0=64$ mV) just slightly above the critical circuit potential where the Hopf-bifurcation took place ($V_H=54$ mV).

Figure 4 shows the effect of delayed feedback on the angular frequency of current oscillations for different values of feedback gain K ranging between 0.01 and 0.08. In Figure 4(a), the feedback is very weak ($K=0.01$); as the feedback delay τ is increased, the angular frequency changes in a harmonic manner. When $\tau=T_0=0.77$ s, the feedback has no effect on the dynamics, and the frequency of the oscillations is the same as the natural frequency. With further increasing the feedback delay, there is a cyclic variation of the angular frequency with respect to τ for about three cycles without change, and three more cycles with only a small change in the amplitude of the Ω vs. τ curves. With these relatively small feedback delays ($\tau<4$ s), there is no hysteresis; the angular frequencies obtained with increasing or decreasing the τ values are almost identical. However, at $\tau>4$ s, instead of the expected next cyclic variation, birhythmicity emerges ($\tau_{crit}=4.85$ s) for a small region of feedback delays. The region of birhythmicity becomes wider for the larger delays

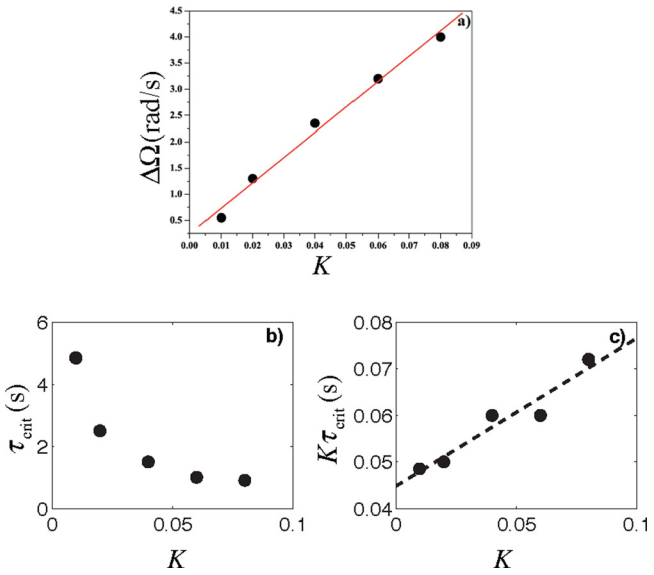

FIG. 6. Experiments: testing the correlations (as predicted by the phase model) between $\Delta\Omega$, K, and τ_{crit} for birhythmicity at weak feedback. (a) The difference between the maximum and minimum of the angular frequencies of the oscillations ($\Delta\Omega = \Omega_{max} - \Omega_{min}$) as a function of the control gain K. The slope of the straight line is $2\beta = 48.38$ rad/s. (b) Critical value of delay time τ_{crit} as a function of the control gain K. (c) $K\tau_{crit}$ as a function of feedback gain K. The slope and the intercept of the fitted line are, respectively, 0.32 s and 0.045 s.

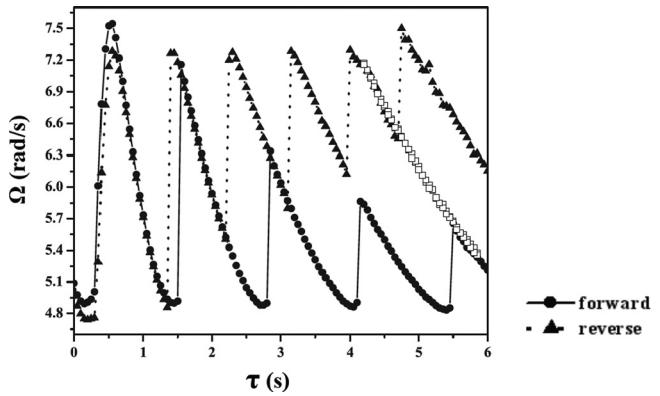

FIG. 7. Experiments: trirhythmicity. Angular frequency of oscillations Ω at large control gain ($K = 0.12$) when the delay time is first increased (●) from 0 to 6 s then decreased back to 0 s (▲). $V_H = 120$ mV, $V_0 = 130$ mV, $R = 87$ Ohm; $T_0 = 1.24$ s. Three different oscillatory modes were observed at large feedback delay ($\tau > 4$ s). Oscillations with angular frequencies corresponding to the middle branch of the diagram (trirhythmicity, □) could be approached by perturbing the system from either the upper or lower branches. The points of the middle branch were traced by either increasing or decreasing the feedback delay τ after the perturbation.

(e.g., $\tau > 5.5$ s). Nonetheless, with the weakest feedback gain ($K = 0.01$), the regions of birhythmicity are very small.

For the stronger feedbacks in Figure 4(b) ($K = 0.02$) and 4(c) ($K = 0.04$), we observed that as the feedback gain is increased, the first critical value of the feedback delay is decreased ($\tau_{crit} = 2.5$ s and 1.5 s, respectively), and the region of birhythmicity is becoming increasingly wider. At even larger feedback gains, "splitting" of the lower and upper branches takes place (see Figures 4(c)–4(e)). The larger the gain the smaller the feedback delay where the first splitting occurs. As a consequence of the splitting of the two branches, during forward scan of τ, instead of the transition from the lower branch (slower oscillations) to the upper branch (faster oscillations), the system rather jumps to the next lower branch (slower oscillations). Similarly, during a reverse scan of τ, the transition from the upper branch (faster oscillations) does not take the system to the lower branch (slower oscillations) but to the previous upper branch (faster oscillations). Notice that similar splitting was also found in the numerical modeling (see Figure 1) at large delays.

Birhythmicity is the result of the coexistence of two stable limit cycles with different periods. The two co-existence current oscillations, shown in Figure 5, were measured in the range of birhythmicity at exactly the same conditions (corresponding to Figure 4(b)). The thick curve belongs to the lower branch (slower oscillations, $T = 0.79$ s), while the thin curve shows the faster oscillations ($T = 0.71$ s) observed during the reverse scan of τ. Note that the applied delayed feedback has only a small effect on the amplitude of oscillations (about 3% variation). However, there is a pronounced, about 11% difference between the periods of the oscillatory curves. This finding indicates that as outlined earlier, a simple phase model could be justifiably applied to explain and characterize the origin of multirhythmicity, at least, with weak feedback gains.

According to Eq. (22), the difference between the maximal and minimal values of the angular frequencies ($\Delta\Omega = \Omega_{max} - \Omega_{min}$) is linearly proportional to the (weak) feedback gain K. This relationship is tested with the experimental data in Figure 6(a). The slope of the straight line is $2\beta = 48.38$ rad/s, that is, the conversion factor $\beta = 24.19$ rad/s. In Figure 6(b), we plot the critical value of feedback delay τ_{crit} as a function of the control gain K (data are taken from Figure 4). Figure 6(b) shows an inverse (hyperbolic) relationship between τ_{crit} and K, suggesting that $K\tau_{crit}$ is nearly constant, as it has been predicted by the phase model. Figure 6(c) shows the $K\tau_{crit}$ values as a function of K. While the K values are increased almost tenfold (from 0.01 to 0.08), the values of $K\tau_{crit}$ increase by ~50% only; therefore, it is possible to approximate the critical feedback delay by determining the value of $K\tau_{crit}$ at a given feedback gain only. Figure 6(c) also shows that the $K\tau_{crit}$ varies nearly linearly as a function of K. The intercept of a linear fit predicts a lower limit $K\tau_{crit} = 0.045$ s for week feedback. This limiting value can be also approximated from the slope of $\Delta\Omega$ vs. K graph shown in Figure 6(a), that is 1 rad/$\beta = 0.0413$ s. As we have discussed earlier, the value of $K\tau_{crit}$ may slightly depend on the value K, too. The lower bound approximation according to Eq. (17) predicts a zero slope for the $K\tau_{crit}$ vs. K graph, while the upper bound approximation according to Eq. (20) gives a slope that is equal to T_0. When changing the delay, sometimes the lower, sometimes the upper bound approximation works better (see Figure 2(c)). Accordingly, the experimentally determined slope (0.32 s) is between 0 and $T_0 \approx 0.75 - 0.8$ s (Figure 6(c)). These quantitative agreements between predictions and experiments indicate that a simple phase model approximation is an effective tool (with excellent predictive power) for characterizing the emergence of birhythmicity.

Both modeling studies predicted (see Figures 1 and 2(a)) that at strong feedback and large delay, there is a possibility

for trirhythmicity. Following the strategy developed by the numerical simulations, we have found the trirhythmicity in the experiments (see the middle branch in Figure 7). The third mode of oscillations could be found by perturbing the system (by slightly changing the circuit potential for a short period of time) from either the upper or lower branches of the oscillations in the region where splitting of the branches occurs; after establishing the new stable oscillations, the middle branch could be traced by increasing and decreasing the feedback delay τ (see Figure 7).

III. CONCLUDING REMARKS

The experiments revealed that the oscillatory electrodissolution of copper under potentiostatic conditions can exhibit multirhythmic behavior when delayed feedback is applied to the circuit potential. With small feedback gain (K) and delay ($0 < \tau < T$), the frequency of oscillations changes only in a nearly harmonic manner. In this region, the difference between the maximum and minimum values of the frequencies can be used to predict the critical delay τ_{crit} that should be applied to induce birhythmicity when high and low frequency oscillations co-exist for the same K and τ. The nearly constant value of $K\tau_{crit}$ implies that a simple phase model approximations can be used predictively for the experiments even at larger delays and gains. We have also showed that feedback could also generate trirhythmicity when three stable periodic orbits with different frequencies can co-exist. Although birhythmicity has been reported in oscillating chemical systems,[25] higher order rhythmicities with single chemical oscillators are difficult to obtain without feedback. The feedback systems thus could provide a convenient way for generating multiple attractors in a chemical system; other possibilities include the application of a forced oscillator with multiple frequency waveforms,[41] or oscillators could be coupled in a mechanism dependent specific manner that produces a phenomenon of extreme multistability.[42]

Because of the generality of the applied phase model, it is expected that multirhythmic behavior can also occur in a wide variety of chemical and biological systems oscillating close to a Hopf bifurcation and subjected to weak, but largely delayed feedback. Most notably, the validity of the phase model approximation at large delays could open a way of extension of synchronization engineering[16,39,43,44] methods to large delays, and, for example, to generate a system with large number of periodic solutions whose frequencies cover a relatively large range. Such system could exhibit entrainment to large range of external signal frequencies, a property of which is an important characteristic of adaptive biological systems, such as the self-tuned oscillator in the human auditory system.[45]

ACKNOWLEDGMENTS

We would like to thank Irving R. Epstein for his pioneering and inspirational work on coupled chemical oscillators, for his encouragement of our activities in nonlinear chemical dynamics, for being an open person we could always turn to, and for his insightful remarks on our work for many years. The work by V. Gaspar and his coworkers (T. Nagy and E. Verner) was supported by Hungarian OTKA Grant No. 81646 and by the TÁMOP 4.2.1./B-09/1/KONV-2010-0007 Project. The project has been implemented through the New Hungary Development Plan, co-financed by the European Social Fund and the European Regional Development Fund. I. Z. Kiss acknowledges support from National Science Foundation under Grant No. CHE-0955555.

[1]M. C. Mackey and L. Glass, Science **197**, 287 (1977).
[2]T. Roenneberg and M. Merrow, J. Biol. Rhythms **14**, 449 (1999).
[3]I. Fischer, G. H. M. van Tartwijk, A. M. Levine *et al.*, Phys. Rev. Lett. **76**, 220 (1996).
[4]K. Pyragas, Phys. Lett. A **170**, 421 (1992).
[5]B. R. Andrievskii and A. L. Fradkov, Autom. Remote Control (Engl. Transl.) **64**, 673 (2003).
[6]E. Schöll and H. G. Schuster, *Handbook of Chaos Control* (John Wiley & Sons, 2008).
[7]I. Z. Kiss and J. Hudson, AIChE J. **49**, 2234 (2003).
[8]A. Mikhailov and K. Showalter, Phys. Rep. **425**, 79 (2006).
[9]E. C. Zimmermann, M. Schell, and J. Ross, J. Chem. Phys. **81**, 1327 (1984).
[10]F. W. Schneider, R. Blittersdorf, A. Forster *et al.*, J. Phys. Chem. **97**, 12244 (1993).
[11]M. Kim, M. Bertram, M. Pollmann *et al.*, Science **292**, 1357 (2001).
[12]I. Z. Kiss, T. Nagy, and V. Gáspár, in *Handbook of Solid State Electrochemistry II*, edited by V. V. Kharton (Wiley-VCH, Weinheim, 2011), p. 125.
[13]I. Z. Kiss, V. Gáspár, and J. Hudson, J. Phys. Chem. B **104**, 7554 (2000).
[14]P. Parmananda, R. Madrigal, M. Rivera *et al.*, Phys. Rev. E **59**, 5266 (1999).
[15]V. S. Zykov and H. Engel, Physica D **199**, 243 (2004).
[16]I. Z. Kiss, C. G. Rusin, H. Kori *et al.*, Science **316**, 1886 (2007).
[17]A. F. Taylor, M. R. Tinsley, F. Wang *et al.*, Angew. Chem. Int. Ed. **50**, 10161 (2011).
[18]W. Wang, I. Z. Kiss, and J. L. Hudson, Phys. Rev. Lett. **86**, 4954 (2001).
[19]M. R. Tinsley, S. Nkomo, and K. Showalter, Nat. Phys. **8**, 662 (2012).
[20]V. K. Vanag, L. F. Yang, M. Dolnik *et al.*, Nature **406**, 389 (2000).
[21]S. Yanchuk and P. Perlikowski, Phys. Rev. E **79**, 046221 (2009).
[22]T. Erneux and J. Grasman, Phys. Rev. E **78**, 026209 (2008).
[23]J. Weiner, R. Holz, F. W. Schneider *et al.*, J. Phys. Chem. **96**, 8915 (1992).
[24]C. Beta, M. Bertram, A. Mikhailov *et al.*, Phys. Rev. E **67**, 046224 (2003).
[25]M. Alamgir and I. R. Epstein, J. Phys. Chem. **88**, 2848 (1984).
[26]B. R. Johnson, J. F. Griffits, and S. K. Scott, J. Chem. Soc. Faraday Trans. **87**, 523 (1991).
[27]A. Goldbeter, in *Biochemical Oscillations and Cellular Rhythms* (Cambridge University Press, Cambridge, UK, 1996).
[28]F. N. Albahadily and M. Schell, J. Chem. Phys. **88**, 4312 (1988).
[29]I. Z. Kiss, Z. Kazsu, and V. Gáspár, Chaos **16**, 033109 (2006).
[30]I. Z. Kiss, Y. Zhai, and J. L. Hudson, Phys. Rev. Lett. **94**, 248301 (2005).
[31]M. T. M. Koper and P. Gaspard, J. Chem. Phys. **96**, 7797 (1992).
[32]M. T. M. Koper, "Oscillations and complex dynamical bifurcations in electrochemical systems," in *Advances in Chemical Physics*, edited by I. Prigogine and S. A. Rice (1996), Vol. XCII, pp. 161–298.
[33]R. Vidal and A. C. West, "Copper Electropolishing in Concentrated Phosphoric Acid I. Experimental Findings," J. Electrochem. Soc. **142**(8), 2682–2689 (1995).
[34]R. Vidal and A. C. West, "Copper Electropolishing in Concentrated Phosphoric Acid II. Theoretical Interpretation," J. Electrochem. Soc. **142**(8), 2689–2694 (1995).
[35]L. T. Tsitsopoulos, I. A. Webster, and T. T. Tsotsis, Surf. Sci. **220**, 391 (1989).
[36]I. Z. Kiss, Z. Kazsu, and V. Gáspár, Phys. Chem. Chem. Phys. **11**, 7669 (2009).
[37]M. Urvölgyi, V. Gáspár, T. Nagy *et al.*, Chem. Eng. Sci. **83**, 56 (2012).
[38]I. Z. Kiss, Z. Kazsu, and V. Gáspár, J. Phys. Chem. A **109**, 9521 (2005).
[39]H. Kori, C. G. Rusin, I. Z. Kiss *et al.*, Chaos **18**, 026111 (2008).
[40]Y. Kuramoto, *Chemical Oscillations, Waves, and Turbulence* (Oxford University Press, Oxford, 1998).
[41]M. Rivera, P. Parmananda, and M. Eiswirth, Phys. Rev. E **65**, 025201 (2002).
[42]C. Ngonghala, U. Feudel, and K. Showalter, Phys. Rev. E **83**, 056206 (2011).
[43]C. G. Rusin, H. Kori, I. Z. Kiss *et al.*, Philos. Trans. R. Soc., A **368**, 2189 (2010).
[44]C. G. Rusin, I. Tokuda, I. Z. Kiss *et al.*, Angew. Chem. Int. Ed. **50**, 10212 (2011).
[45]F. Julicher, D. Andor, and T. Duke, Proc. Natl. Acad. Sci. U.S.A. **98**, 9080 (2001).